Role of Force Resultant Interaction on Ultra-High Performance Concrete

Author(s) & Affiliation:

Titchenda Chan (1), Kevin R. Mackie (1), and Jun Xia (2)
(1) Civil, Environmental, and Construction Eng. Dept., University of Central Florida, Orlando, Florida
(2) Civil Eng. Dept., Xi'an Jiaotong-Liverpool University, Suzhou, Jiangsu, China

Abstract:

With considerably high strength and high ductility due to the fiber bridging effect, ultra-high performance concrete (UHPC) beams can be designed without shear reinforcement. This could make UHPC beams shear critical members when high-strength flexural reinforcement is used. Classical uniaxial moment-curvature analysis would overestimate stiffness and capacity of the elements in the case of shear critical behavior. Stiffness reduction is often introduced by adding shear deformations, while beam capacity is reduced through the introduction of new shear strength design formulas or based on uniaxial normal stress level. However, this adjustment does not precisely explain the underlying causes of shear failure of the UHPC beams. The purpose of this research is to quantify the force resultant interaction of UHPC flexural members as well as their failure modes by using available biaxial stress state analysis approaches such as modified compression field theory (MCFT) and the finite element method. The load-displacement results are compared with moment-curvature analysis. Various experimental specimens were tested to validate the analytical results including unreinforced UHPC prisms, UHPC prisms reinforced with ASTM Grade 60, and UHPC prisms reinforced with high strength steel (HSS). Flexural failure was observed on unreinforced UHPC and UHPC-Grade 60 steel reinforced specimens, where the crack opening gradually widened at the bottom layer of the concrete below the loading position. On the other hand, UHPC-HSS specimens largely failed in shear from a diagonal tension crack and crushing of concrete top layer. The accuracy as well as the limitations of the analysis methods used are identified and discussed based on experimental test results.

Keywords: Moment-curvature analysis, modified compression field theory, flexural test, high strength steel rebar

1. Introduction

Ultra-high performance concrete (UHPC) is a cement matrix material having compressive strength higher than 22 ksi (150 MPa) as defined by Association Francaise de Genie Civil (AFGC 2002). Special characteristics of UHPC are its strain-hardening effects and ductile behavior due to the 2% volume-fraction steel fibers under tensile stress. Although the water content of UHPC is low, appropriate granular packing plus the addition of a high-range water reducing admixture ensures its good rheological properties. UHPC material has been used in numerous construction projects such as highway and pedestrian bridges, buildings, and other infrastructure projects. A few commercially available UHPC premixes are available in the US market, and one of them developed by Lafarge is used in the study discussed.

Numerical nonlinear analysis, especially using the finite element method, is widely used to investigate the structural behavior of reinforced concrete components. For the case of reinforced concrete beams, several approaches are available, which may or may not consider the force resultant interaction. One-dimensional (sectional) moment-curvature analysis, in which beam sections are discretized into many layers, is a commonly used method for analysis of RC beams, because the method is very simple and robust. However, it is a uniaxial stress approach that neglects the effects of shear stress. One-dimensional sectional modified compression field theory (MCFT) (Vecchio 1988) on the other hand is a smeared rotating biaxial stress approach considering interaction of axial force, bending moment, and shear force effects through Mohr's circle. The angles of principal stresses and strains are assumed to be equal. Two-dimensional membrane finite element analysis (FEA) based on continuum methods using MCFT as implemented in VecTor2 software (Wong 2013) is another possible analysis option.

2. Background

UHPC beams reinforced with high strength steel (HSS) have been investigated as a potential solution for moveable bridge decks. Its lightweight and satisfactory strength under traffic load has been demonstrated (Saleem 2012). During the test of simply-supported deck strips, shear-flexural failure was identified as the dominant failure mode for most of the specimens, shown in Figure 1, despite the inclusion of different reinforcement configurations. In addition, the failures were ductile involving large deformation and large sectional rotation.

Xia (2011) studied the shear failure of small UHPC-HSS prisms and the deck strips, as well as their force resultant interaction. To achieve the maximum allowable shear stress, a moment-curvature analysis was used to determine the normal stress level of each beam layer, after which different principal stress interaction models were employed. Although the cause of shear failure was still unclear from the results, the shear stresses considerably degraded the capacity of the elements. To explain such non-conventional shear failure modes, it is important to employ a biaxial stress analysis where both normal and shear stresses are included.

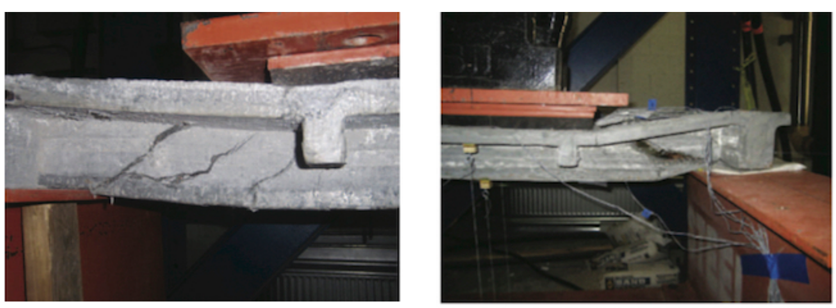

Figure 1. Failure Modes of UHPC-HSS With and Without Stirrups (Xia 2011)

3. Testing Methods

3.1. UHPC Materials Used

The UHPC used in this research is the Ductal-UHPC premix developed by Lafarge, whose high compressive strength is achieved by finely graded granular materials and water-cement ratio as low as 0.2. The average dimension of fine sand is between 150 and 600 µm, while those for cement and crushed quartz are around 15 µm and 10 µm, respectively. Silica fume is used to fill the void spaces between those aggregates. Extra super-plasticizer is required to obtain better workability. Steel fibers (2% by volume) with the length of 0.5 in (12.7 mm) and diameter of 0.008 in (0.2 mm) having yield strength of 3150 MPa are used to increase the UHPC tensile strength and bridging effect. Ice and a high shear mixer were used for UHPC mixing to ensure better homogeneity. The proportion of constituent materials as well as its mixing procedure follows Graybeal (2006).

3.2. UHPC Prism Specimens

To investigate the shear failure mode, several groups of specimens with different cross-sectional areas, shear-span ratios, and reinforcement types as shown in Table 1 were tested under three-point bending load. The specimen configurations are illustrated in Figure 2.

Table 1. Specimen Description

	Width (mm)	Height (mm)	Span (mm)	Rebar size	Rebar Type	Quant.
G1	51	51	305	-	No	3
G2	38	102	660	#3,	G60	3
G3	38	102	457	#3,	G60	3
G4	38	76	305	#3,	HSS	3
G5	38	76	457	#3,	HSS	3
G6	38	76	610	#3,	HSS	3

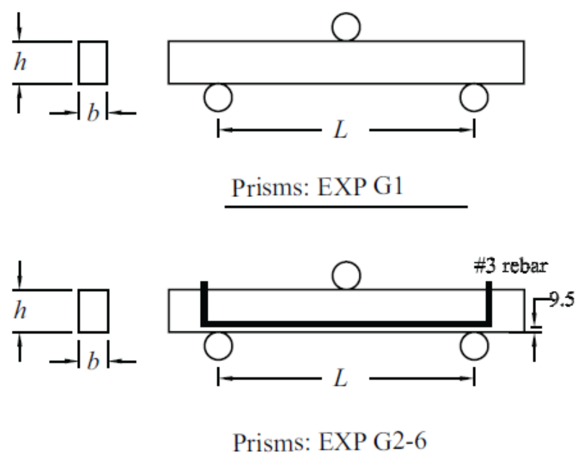

Figure 2. Specimen Setups

3.3. Raw material properties of UHPC and Steel Reinforcement

Cast in two different batches, G1-G3 and G4-G6 specimens were tested conforming to ASTM C39 and had a compressive strength of 21 ksi (145 MPa) and 23 ksi (160 MPa), respectively. However, UHPC's first crack and ultimate tensile strengths of 1.16 ksi (8 MPa) were adopted from previous UHPC studied specimens (Graybeal 2006) with similar compressive strength due to the limitation of accurate testing equipment. On the other hand, the tension test of HSS and Gr. 60 steel conforming to ASTM E8 showed their yield strength of 165 ksi (1138 MPa) and 60 ksi (414 MPa), and ultimate strength of 165 ksi (1138 MPa) and 105 ksi (723 MPa), respectively.

4. Experimental Results

The test results (Figure 3) showed that all unreinforced and Gr. 60 steel reinforced specimens failed in flexure with large crack openings at mid span. However, based on the load-displacement diagrams in Figure 4, failures of G2 and G3 specimens were more ductile than G1 specimens due to the yielding of reinforcement. On the other hand, most of HSS-reinforced specimens failed in shear with large diagonal tension crack and crushing of concrete top layers even though the shear span ratio of G6 specimens is 4.33. Exceptionally, one specimen in G6 exhibited a more ductile shear failure based on its load-displacement (Figure 4f).

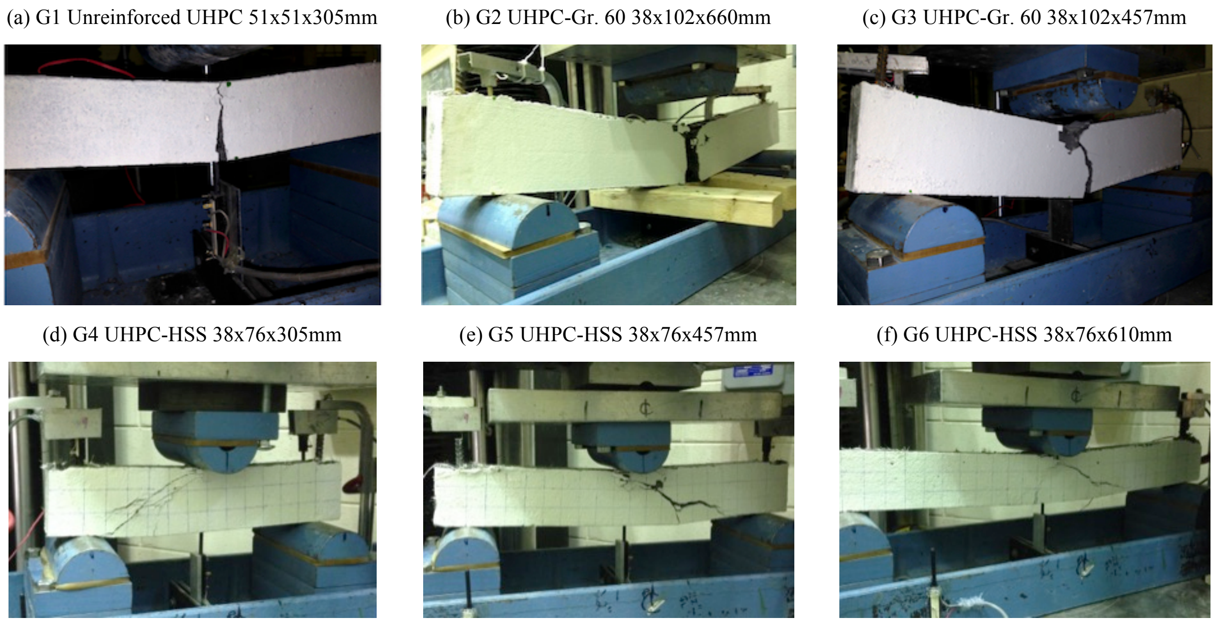

Figure 3. G1-G6 Typical Failure Modes

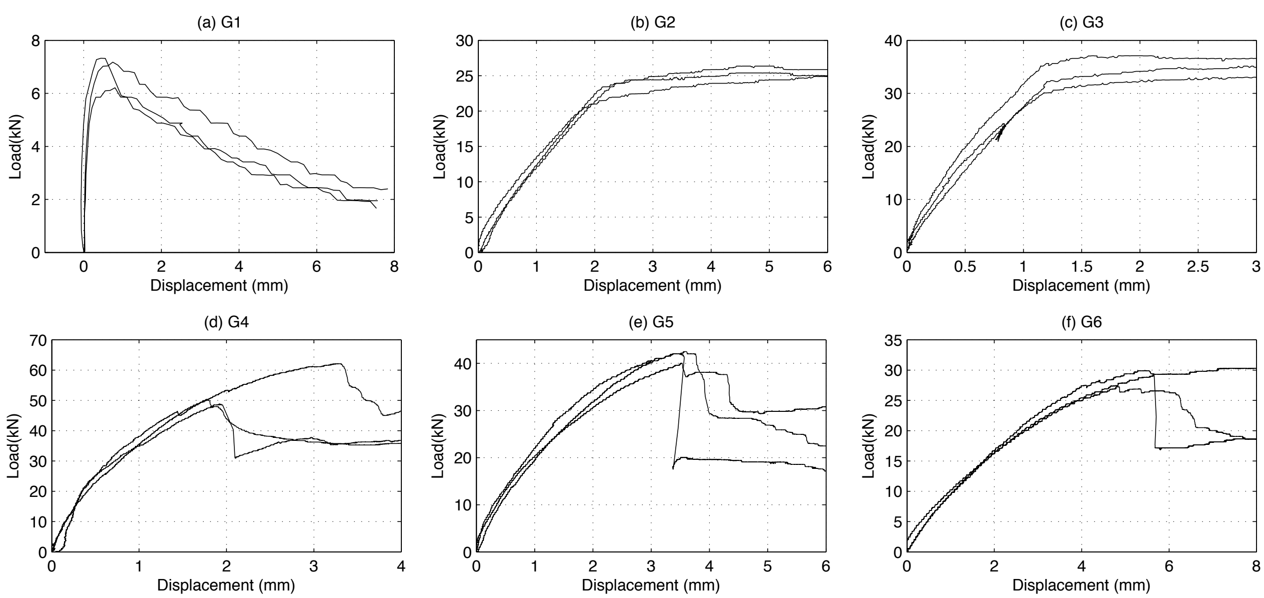

Figure 4. G1-G6 Experimental Load-Displacement

5. Analysis Methods

5.1. Sectional Analysis: Moment Curvature

One dimensional moment-curvature (M-Phi) analysis is a layer-based sectional analysis method with nonlinear material constitutive models for each material in a composite section. The load-displacement behavior of RC beams can be obtained by integration of multiple such sections along the beam length. With the imposed global displacement, a sectional curvature and axial strain of each section can be determined through the classical planar section compatibility assumption. Axial stresses corresponding to axial strains from the nonlinear uniaxial stress-strain models of all RC layers are obtained by satisfying the equilibrium between compression and tension forces within each section. The corresponding sectional bending moment can, therefore, be determined with those known concrete and rebar layer stresses. The method is very robust to get convergence; however, its obvious drawback is it neglects shear stress and shear deformation effects, slip, and no crack orientation is considered.

5.2. Sectional Analysis: MCFT

MCFT is based on a rotating smeared crack concept that considers the orthotropic nonlinear constitutive relation of cracked concrete. Concrete crack orientations in MCFT vary as the loading intensity changes. MCFT considers the interaction of all resultant forces (normal, shear, and bending moment) and can be applied to one-dimensional and two-dimensional analyses. Similar to moment curvature, one-dimensional MCFT follows layer-based sectional analysis in which all beam sections need to satisfy constitutive relations, equilibrium, and compatibility requirements. However, the last two requirements are more complicated involving the inclusion of shear stress and strain by accounting for the angle of inclination of principal stress/strain via Mohr's circle. An essential assumption in MCFT is that the angles of inclination of principal stress and strain are equal.

At the global level, this sectional MCFT was integrated with nonlinear analysis program NAP (Mackie 2011), and displacement-based elements were used for faster convergence. Using displacement-based elements, it is necessary that the displacement and curvature field along the element are determined from the same shape functions and their derivatives. Because no shear strains or rotations of the beam relative to its section are predicted in Euler-Bernoulli flexural theory, an approximate shear strain field was taken from the third derivative of the same shape functions. This results in constant shear strain within each element (Figure 5a); however, by using 6 elements for one beam, a good representative shear strain distribution can be obtained. Detailed derivations can be found elsewhere (Chan 2014). Additionally, Guner (2008) realistically simulated the response and failure modes for normal RC beam with two extra assumptions that were also adopted: parabolic shear strain along section depth (Figure 5b) and zero vertical stress.

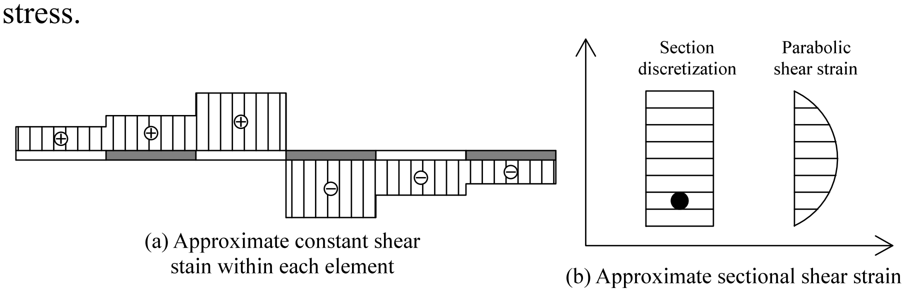

Figure 5. Approximate Elemental and Sectional Shear Strains

5.3. Two-Dimensional Finite Element Analysis: MCFT Using VecTor2

The two-dimensional (2D) MCFT finite element analysis (FEA) (Vecchio 1990) is based on the classical plane stress displacement-based finite element method. It incorporates a system of equations involving approximate nodal displacements, applied forces, and the structure stiffness matrix. Different from conventional plane stress FEA where the material tangent stiffness is used and convergence is reached when residual nodal displacements are infinitesimal, 2D MCFT based FEA utilizes an iterative secant stiffness formulation and uses secant moduli as the convergence criteria. The benefits of using 2D plane stress MCFT over the one-dimensional sectional MCFT are that both approximate axial and shear strain fields of each element can be obtained at once from the global displacement through shape functions. Also, no assumption of zero vertical stress is needed. VecTor2, a plane stress implementation of MCFT for RC analysis (Wong 2013), was used in research analysis. In this MCFT-VecTor2 modeling, four-noded rectangular elements with uniform thickness were used to model the UHPC; 2D truss element was used to model rebar, and the perfect bond between UHPC and rebar was assumed.

5.4. Failure Criteria

Flexural failure for simply-supported beams can be identified from the results of classical moment-curvature analysis if the rebar strain exceeds its yielding strain. Shear failure can be identified by large compressive strains along the compression strut. For MCFT, besides the failure modes identified from normal strains, failure modes in MCFT can also be investigated via principal tensile/compressive strains determined from the combination of axial and shear strains (biaxial state). Large principal compressive strain along the compression strut can be used to detect shear failure of deep beams; while principal tensile strain and its angle are helpful inputs to find shear cracks of shallow beams.

5.5. Materials Constitutive Models for the Analyses

In both 1D and 2D analyses, the Hognestad model (Wong 2013) was adopted for the constitutive behavior of concrete in compression, and Vecchio-Collins 1982 (Wong 2013) was used for concrete compression softening. For concrete in tension, 1D MCFT analysis uses a tri-linear stress-strain curve, which is the simplified tensile response of Graybeal's UHPC specimen F2A-Long (Graybeal 2006). The 2D analysis combined the available exponential tension-softening model with simplified diverse embedment model (SDEM-monotonic) (Wong 2013). On the other hand, HSS used a curve-fit stress-strain relation following the relation $f_s(MPa) = 1138(1 - e^{-236.27e_s})$. ASTM Gr. 60 steel used tri-linear elastic-hardening curve with offset strain of 0.006 and failure strain of 0.06.

6. Analysis Results

6.1. One Dimensional Nonlinear Analysis Based on MCFT

The sectional MCFT analysis provided good predictions of load-displacement responses when compared with the test results; however, with regard to the failure modes, flexural failures were only observed for specimens from G1, G2, and G3. Unreinforced UHPC specimens of G1 typically exhibited flexural failure due to the drop of tensile strength at the bottom layers of the prisms. After the tensile strain reached the softening branch, the angle of inclination was almost 0º. Flexural failures for G2 and G3 specimens were observed due to yielding of reinforcement as indicated by the horizontal line of the load-displacement diagram in Figure 6a. These flexural failure modes could also be identified through the largest principal tensile strain (e_1) of the bottom layer at mid span (@L/2). However, despite a clear match in the load-displacement curve for G5 specimens, the method did not indicate shear failure because the principal tensile strains were still the largest at the bottom layers at mid span (Figure 6b). Also, the load-displacement determined from moment-curvature analysis was found to have only slightly stiffer responses. Reasons behind the shortcomings in predicting the failure modes are discussed in the conclusions.

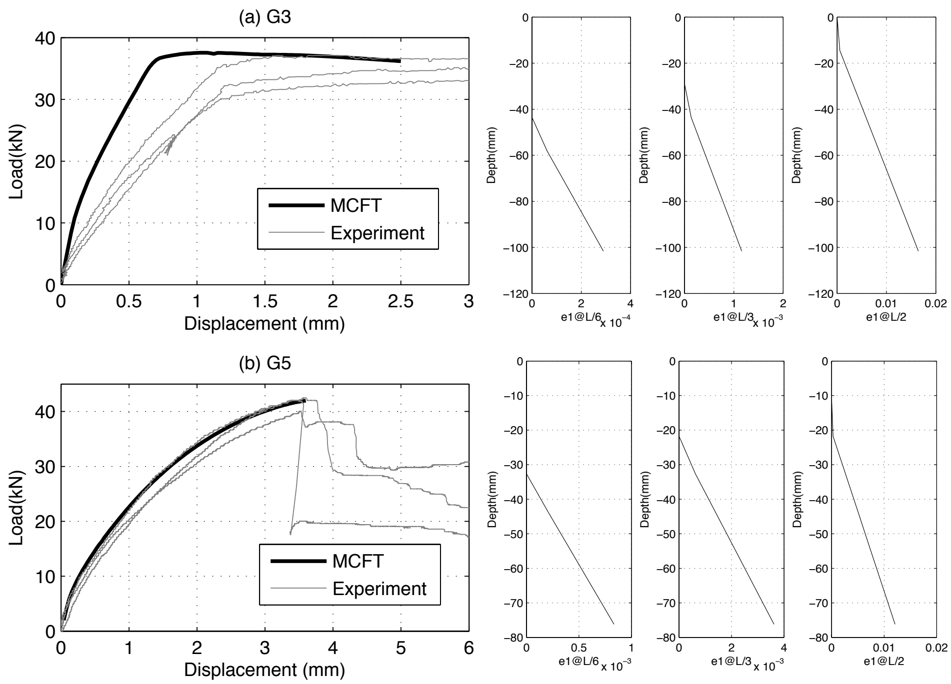

Figure 6. G3 and G5 MCFT Load-Displacement and Principal Tensile Strain at the Peak

6.2. Two Dimensional Nonlinear FEA Based on MCFT (VecTor2)

The 2D MCFT implemented in VecTor2 software gave very similar results to the tests for both load-displacement response and failure modes. Figure 7a-7c illustrated one typical result of load-displacement and diagonal tension shear crack from VecTor2. The flexural failures of G1 specimens, whose cracks were almost vertical lines, were due to the same mechanism as explained in MCFT sectional analysis. However, the flexural cracks of G2 and G3 specimens deviated slightly from the vertical lines due to the presence of Gr. 60 reinforcement. The G4, G5, and G6 specimens failed in diagonal tension shear because HSS reinforcement provided sufficiently high tensile strength (yielding of HSS was not observed), which keeps the mid-span principal tensile strain and angle of inclination low. As the load increased, the principal tensile strain and its angle of inclination on both sides of the mid span turned to 45º from the loading point. The strain values increased rapidly due to the lack of a stirrup. Finally the concrete failed in shear as indicated in Figure 7c. Despite indicating a shear failure at the peak load, VecTor2 did not show small shear cracks at lower load levels that were observed during the experimental tests.

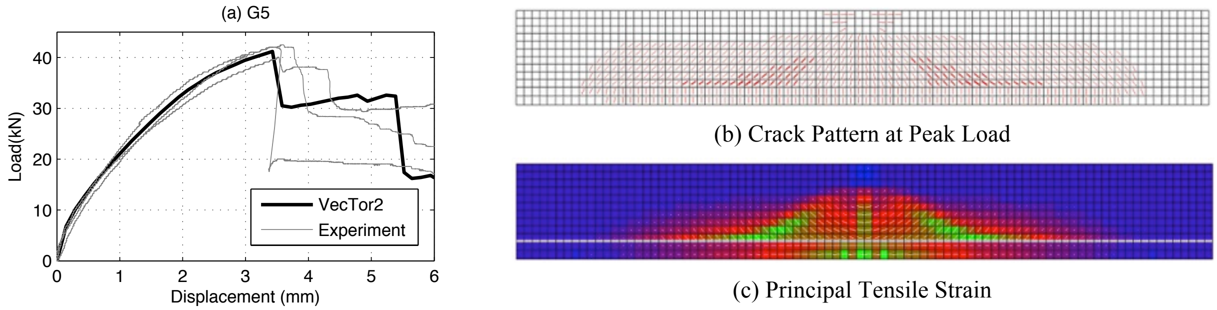

Figure 7. G5 VecTor2 Load-Displacement, Crack Patterns, and Principal Tensile Strain

7. Discussion and Conclusion

Both nonlinear structural analysis (with one-dimensional displacement-based elements and a sectional MCFT implementation) in the program NAP and nonlinear finite element analysis (plane stress based on MCFT) using VecTor2 software can effectively predict the load-displacement responses of UHPC prisms with different types of flexural reinforcement. However, the 1D MCFT had difficulty in capturing the shear failure modes, and by comparing to moment-curvature analysis, a slight weaker load-displacement response was observed. These problems were possibly caused by the assumption of zero vertical stress and no local shear cracks. The 2D-MCFT using VecTor2 captured both flexural and shear failures. The shear failures of UHPC-HSS prisms were caused by the presence of high tensile strength of HSS that did not yield, which maintains low principal tensile strain and small angle of inclination at mid span. The shear crack can develop prior to the flexural crack because the absence of stirrups in the prisms where the angle of inclination was high (45º degree from the loading position).

8. References

Association Francaise de Genie Civil, "Ultra High Performance Fibre-Reinforced Concretes," *Interim Recommendations*, Paris, France 2002.

Chan, T., "Role of Force Resultant Interaction on Fiber Reinforced Concrete," *MS Thesis*, University of Central Florida, Orlando, Florida, 2014.

Graybeal, B. A., "Material Property Characterization of Ultra-High Performance Concrete," *Report No. FHWA-HRT-06-103*, FHWA, U.S. Department of Transportation, August 2006.

Mackie, K., "Nonlinear Analysis Program (NAP)," Nonlinear Structural Analysis, University of Central Florida, Orlando, Florida, 2011.

Saleem, M. A., Mirmiran, A., Xia, J. and Mackie, K., "Ultra High Performance Concrete Bridge Decks Reinforced with High-Strength Steel or Fiber Reinforced Polymers," *ASCE Structures Congress*, 2012, pp. 718 – 734.

Vecchio, F. J., "Reinforced Concrete Membrane Element Formulations," *ASCE Journal of Structural Engineering*, Vol. 116, No. 3, 1990, pp. 730-750.

Vecchio, F. J. and Collins, M. P., "Predicting the Response of Reinforced Concrete Beams Subjected to Shear Using Modified Compression Field Theory," *ACI Str. J.*, 85, 1988, 258-268.

Wong, P., Trommels, H. and Vecchio, F. J., "VecTor2 and Formwork Manual," August 2013.

Xia, J., Mackie, K., Saleem, M. A., Mirmiran, A., "Shear Failure Analysis on Ultra-High Performance Concrete Beams Reinforced with High Strength Steel" *Eng Str.33*, 2011, 3597-609.